第 49 卷第 2 期　　硅　酸　盐　学　报　　Vol. 49，No. 2
2021 年 2 月　　JOURNAL OF THE CHINESE CERAMIC SOCIETY　　February，2021
http://www.gxyb.cbpt.cnki.net　　**DOI**：10.14062/j.issn.0454-5648.20200476

负载银纳米立方体的醋酸纤维素纳米纤维及其 SERS 活性

柯　岩[1,3]，陈　斌[1]，周宁宁[1]，黄竹林[1]，孟国文[1,2]

(1. 中国科学院合肥物质科学研究院，固体物理研究所，材料物理重点实验室和安徽省纳米材料与技术重点实验室，合肥 230031；2. 中国科学技术大学化学与材料科学学院 合肥 230026；3. 广东溢达纺织有限公司，广东 佛山 528500)

摘　要：报道了一种采用同轴静电纺丝法制备的表面增强 Raman 散射(SERS)活性衬底，用于微量环境污染物的快速检测。采用醋酸纤维素(CA)/丙酮-二甲基乙酰胺溶液作为前驱液分散银纳米立方体，利用丙酮促进银颗粒适度团聚，采用同轴静电纺丝法制备了大面积银立方体/CA 纳米纤维。由于团聚态银纳米立方体之间的等离子体耦合作用，复合薄膜具有优异的 SERS 活性，是单分散态的银立方体/CA 纳米纤维 SERS 灵敏度的 4 倍，实现了 0.1 nmol/L 的对巯基苯胺以及 10 nmol/L 的甲基对硫磷农药的 SERS 检测，SERS 信号强度偏差小于 12%。

关键词：表面增强拉曼散射；银纳米方块；纳米纤维；静电纺丝
中图分类号：0433　　**文献标志码**：A　　**文章编号**：0454–5648(2021)02–0220–09
网络出版时间：2020–10–23



Surface-enhanced Raman Scattering from Electrospun Cellulose Acetate Nanofibers Loaded with Aggregated Ag-nanocubes

KE Yan[1,3], *CHEN Bin*[1], *ZHOU Ningning*[1], *HUANG Zhulin*[1], *MENG Guowen*[1,2]

(1. Key Laboratory of Materials Physics and Anhui Key Laboratory of Nanomaterials and Technology, Institute of Solid State Physics, HFIPS, Chinese Academy of Sciences, Hefei 230031, China; 2. School of Chemistry and Materials Science, University of Science and Technology of China, Hefei 230026, China; 3. Guangdong Esquel Textiles Company Limited, Foshan 528500, Guangdong, China)

Abstract: Cellulose acetate (CA) nanofibers were embedded with aggregated silver-nanocubes (AgNCs) by a coaxial electrospinning method. AgNCs were dispersed with CA and acetone-dimethylacetamide (DMAc) as a precursor solution, and AgNCs aggregation was induced with acetone. The nanofibers have a remarkable surface-enhanced Raman scattering (SERS) activity due to the strong plasmon coupling between neighboring AgNCs, which is 4 times of the monomeric-AgNC/CA sample. As a result, 0.1 nmol/L *p*-aminothiophenol (*p*-ATP) and 10 nmol/L methyl parathion can be identified, respectively. The nanofibers generate large-area homogeneous SERS signals with a relative signal deviation of less than 12% over 1 mm×1 mm area due to the homogeneous adsorption of target molecules. It is thus indicated that aggregated-AgNCs/CA nanofibers have a promising potential in SERS-based detection of organic pollutants in aqueous solutions.

Keywords: surface-enhanced Raman scattering; Ag-nanocube; nanofiber; electrospinning

1　Introduction

The interaction between light and metal nanostructures leads to localized surface plasmon resonance (LSPR) effect. This unique optical property of metal nanostructures can have numerous applications in the areas of sensors[1], energy conversion[2], imaging[3], photothermal therapy[4–6], seawater desalination[7], plasmon driven photocatalysis[8–10], and surface-enhanced Raman scattering (SERS) based

收稿日期：2020–06–29。　修订日期：2020–08–04。
基金项目：国家自然科学基金(51632009，91963202，21673245)；中科院前沿科学重点研究计划(QYZDJ-SSW-SLH046)；中科院青年创新促进会；安徽省自然科学基金(1908085QE173)。
第一作者：柯　岩(1989—)，男，博士；
陈　斌(1986—)，男，博士，副研究员。
通信作者：孟国文(1960—)，男，博士，研究员；
黄竹林(1984—)，男，博士，副研究员。

Received date: 2020–06–29.　Revised Date: 2020–08–04.
First author: KE Yan (1989–), male, Ph.D.;
CHEN Bin (1986–), male, Ph.D., Associate Professor.
E-mail: keyan@issp.ac.cn; bchen@issp.ac.cn
Correspondent author: MENG Guowen (1960–), male, Ph.D., Professor.
HUANG Zhulin (1984–), male, Ph.D., Associate Professor.
E-mail: gwmeng@issp.ac.cn; zlhuang@issp.ac.cn.

signal amplification[11–13]. For SERS-based molecule detection, it is well established that LSPR induced electromagnetic field enhancement could amplify the Raman signals of adsorbed molecules by 10^4–10^{12} times, which is sufficient for single molecule detection[14–15]. Also, the SERS enhancement exists at the nanogaps or sharp edges of a nanostructure, such as Au and Ag nanoparticles (NPs), nanocubes, nanostars and polyhedral nanocrystals.

The SERS enhancement can be essentially improved when solitary NPs are coupled or aggregated according to the single/few particle SERS measurement[16–17]. A classical approach is to use aggregating agents (i.e., salt and anti-polar solvent), so that giant electromagnetic enhancement can be achieved among the NPs in an aggregate in solution[18–19]. However, a challenge comes with dispersed SERS platform is the signal stability as it is difficult to track the random aggregation in solution and achieve reproducible SERS signals due to the Brownian motion of particles as well as competition between molecule adsorption and diffusion. In this case, researchers turn to solid matrix SERS substrates (i.e., silicon wafer or polymer film) with strongly coupled SERS-active units[20–21]. By using advanced lithographic techniques (*e.g*. nanoimprint lithography, electron and ion beam lithography), Maria Alba, *et al.* reported a template-assisted method to assemble Au nanospheres onto a silicon wafer with inverted periodical pyramid arrays[22]. Thai, *et al*. reported the self-assembly of free standing Au nanorod arrays on a micropatterned silicon wafer[23]. Such SERS substrates consisted of highly ordered arrays of coupled plasmonic NPs could generate strong and reproducible SERS signals. However, developing a simple and cost-efficient method for large-area solid matrix SERS substrates with high SERS activity and good signal reproducibility becomes a challenge.

Electrospinning is a simple, efficient and versatile electrohydrodynamic technique for mass fabrication of high-quality polymer nanofibers[24]. The nanofibers are usually applied in sensors[25], energy[26], filtration[27], and recently in respiratory mask that has a large demond due to the widespread COVID-19[28]. The functions of electrospun nanofibers can be further extended by incorporating functional materials (i.e., carbon materials and metal NPs)[29–30]. For instance, plasmonic Ag nanospheres and Au nanorods[31–32], are planted into electrospun nanofibers as flexible SERS substrates, which can generate large-area homogeneous SERS signals due to the statistically uniform distribution of Au/Ag NPs and efficient adsorption of target molecules. However, the presented SERS sensitivity is seriously restricted by the isolation of plasmonic NPs due to the following reasons. First, in a typical electrospinning process, the solvent system should be selected to accommodate the polymer for a good spinnability. Second, the solvent should also induce slight aggregation of particles to improve SERS sensitivity. However, it is diffficult to balance the aggregation of NPs and dispersion of polymetric matrix. Coaxial electrospinning (co-electrospinning) as a well-known modified electrospinning method, in which two solutions are delivered into the inner and outer channels of a coaxial bi-channel spinneret, respectively[33], could induce electrospun nanofibers with embedded NP aggregates.

In this paper, a simple and low-cost approach was used to prepare co-electrospun cellulose acetate (CA) nanofiber membranes with aggregated Ag nanocubes (AgNCs) embedded in each nanofiber as highly sensitive and reproducible SERS substrates. The aggregation of AgNCs could be controlled by introducing acetone in the solvent system for electrospinning, leading to a significantly improved SERS sensitivity due to the strong plasmon coupling between neighboring AgNCs. Moreover, the CA nanofiber could efficiently promote the adsorption of the hydrophobic organic pollutants in aqueous solutions for efficient SERS detection application owing to the abundant hydroxyl groups on CA polymer chains, excellent hydrophilicity, as well as the pinholes in CA networks to allow the molecules pass through[34–35]. As a result, *p*-aminothiophenol (*p*-ATP, a probe molecule) and methyl parathion (MP, an organophosphorus pesticide) with the concentration down to 0.1 nmol/L and 10 nmol/L could be identified, respectively. In addition, the SERS signal deviation of AgNCs/CA nanofiber membranes for *p*-ATP was measured to be 12.2%, ascribed to the efficient adsorption of target molecules and the average effect of randomly distributed AgNC aggregates inside the CA nanofibers. Thus the aggregated-AgNCs/CA nanofibers show potentials for SERS-based detection of organic pollutants in aqueous environmental samples.

2 Experimental

2.1 Materials and reagents

Cellulose acetate (*Mw*~30,000, 39.8% acetyl groups), pare-aminothiophenol and methyl parathion were purchased from Shanghai Aladdin Reagent Co. Ltd., China N,N-dimethylacetamide, acetone, polyvinylpyrrolidone (PVP), ethylene glycol (EG) were purchased from Sigma-Aldrich Co., USA. Silver nitrate ($AgNO_3$), sodium chloride (NaCl) were obtained from Sinopharm Chemical Reagent Co. Ltd., China All the chemicals were used without further purification. The coaxial spinneret was purchased from Changsha Nano-apparatus Technology Co. Ltd., China.

2.2 Preparation of precursor solution for electrospinning

The CA/acetone-DMAc (3:2, volume fraction) was prepared by dissolving CA (3 g) in 20 mL mixture solvent consisting acetone (12 mL) and DMAc (8 mL). The CA/acetone-DMAc (volume ratio=2:1, the same below) was prepared by dissolving CA (2.25 g) in mixture solvent consisting 10 mL acetone and 5 mL DMAc. The CA/DMAc solution was prepared by dissolving CA (3 g) in 20 mL DMAc solvent. AgNCs

were prepared by a modified polyol reduction method[36]. NaCl was used as an etchant instead of Na_2S. AgNCs (approximately 60–80 mg in one shot of fabrication) were washed with ethanol and water for six times and then redispersed in 0.2 mL DMAc solvent. Afterwards, AgNCs/DMAc colloidal solution was added to 0.8 mL CA/acetone-DMAc (3/2, volume ratio) solution, followed under vigorous sonication for 2 h to obtain a precursor electrospinning solution. A slight aggregation of AgNCs occurred in the static suspension during 6 h. For comparison, 0.2 mL AgNCs/DMAc colloidal solution was mixed with 0.8 mL CA/DMAc solution to prepare CA/DMAc solution with monodispersive AgNCs.

2.3 Preparation of AgNCs/CA nanofibers

The aggregated-AgNCs/CA nanofibers were fabricated by a co-electrospinning method, as shown schematically in Fig. 1. Note that acetone as a poor solvent of AgNCs could induce appropriate aggregation of AgNCs[37]. The aggregated AgNCs dispersed CA/acetone-DMAc solution could be thus prepared by dispersing AgNCs/DMAc colloidals in the CA/acetone-DMAc solution(see Fig. 1(a)-(c)). Subsequently, CA nanofiber membrane with implanted AgNCs could be fabricated by using aggregated-AgNCs/CA/acetone-DMAc solution as a core solution and CA/acetone-DMAc as a shell solution, respectively (see Fig. 1(d)). In detail, the AgNCs/CA/acetone-DMAc (3/2) solution and CA/acetone-DMAc (2/1) solution were fed into the inner and outer channels of a coaxial spinneret as the core and shell solutions, respectively. The flowrates of core and shell solutions both were 0.2 mL/h. The co-electrospinning experiment was carried out at 12 kV high voltage, and 10 cm working distance at RT with ~50% relative humidity. The monomeric-AgNCs/CA nanofibers were fabricated by electrospraying acetone free AgNCs monodispersive CA/DMAc solution at 15 kV high voltage, and 15 cm working distance at RT with ~50% relative humidity at a flowrate of 0.2 mL/h.

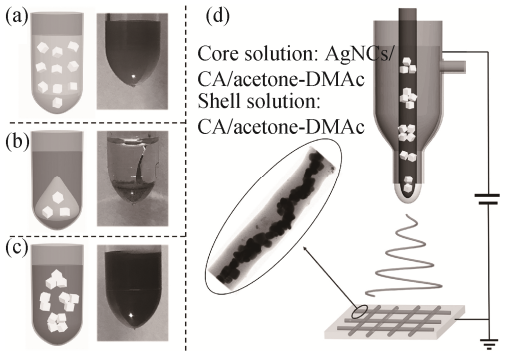


Fig. 1 Schematic illustration for the preparation of AgNCs@NA nanofibers. Optical images of (a) AgNCs/DMAc colloidal suspension, (b) CA/acetone-DMAc solution added with highly-condensed Ag-NCs/DMAc colloidal solution shown in (a), and (c) the mixture obtained after sonication for 6 h. (d) Scheme for the fabrication of AgNCs/CA nanofibers by co-electrospinning method with independent core and shell solution

2.4 Characterizations

AgNCs/CA nanofibers were characterized by a model Cary 5E UV-Vis spectrophotometer (Varian, Australia), a model SU8020 scanning electron microscope (FE-SEM, Hitachi Co. Ltd., Japan) and a model JEM-2010 transmission electron microscope (TEM, JEOL Co., Japan).

2.5 SERS measurement

The as-prepared membranes were firstly tailored to small pieces (5 mm×10 mm), and then the tailored membranes were immersed in aqueous solution of *p*-ATP and MP for 6 h, taken out and dried in air. The substrates were measured by using a confocal Raman spectrometer (Renishaw Invia, UK). All the SERS spectra was measured with 785 nm laser. The acquisition durations were 5 s and 10 s for *p*-ATP and MP, respectively, at a laser power of 0.125 mW. The SERS mapping was measured by using the Renishaw Streamline accessory (line, 50× objective). The acquisition times were 0.25 and 0.5 s for *p*-ATP and MP respectively, at a laser power of 0.25 mW.

3 Results and discussions

3.1 Electrospinning of AgNCs/CA nanofibers

CA as a non-toxic, eco-friendly and renewable polymer with an excellent hydrophilicity is widely used in environmental and biomedical fields[38]. The electrospinning of CA nanofibers is extensively investgated, and the mixture solvent of acetone and DMAc (2/1) is a versatile solvent system for the electrospinning of CA nanofibers[36]. Polyvinylpyrrolidone (PVP) coated AgNCs achieved by a conventional polyol reduction method (see Fig. 1) were used as the plasmonic NPs for their strong Raman enhancement generated at the sharp corners and edges. Moreover, PVP coated AgNCs have a good monodispersity in DMAc solvent. However, they could not be dispersed, readily leading to the aggregation and subsequently precipitation in acetone solvent. Acetone could induce the aggregation of AgNCs[36].

As colloidal AgNCs contact CA/acetone-DMAc solution, AgNCs aggregation occurs (see Fig. 1). Note that AgNCs readily aggregate and even precipitate at a great concentration when dispersed in the mixture solvent of acetone and DMAc (3/2). However, CA solution with a high viscosity can prevent AgNCs from excessive aggregation and further precipitation. It is indicated that CA/acetone-DMAc (3/2) solution could have a good electrospinnability and be electrospun into uniform CA nanofibers (see Fig 2(a)). AgNC aggregates could slightly affect the electrospinnability and spinneret blocking happened frequently. The co-electrospinning technique whithout a highly electrospinnable core solution could be thus used to load aggregated-AgNCs in CA Nanofibers[39]. Large-area homogenous CA nanofibers with AgNC aggregates embedded in nanofibers could be obtained by this technique.

3.2 Characterization of the AgNCs/CA nanofibers

The aggregated-AgNCs/CA nanofibers show grey color (Fig. S2), suggesting the aggregates are indeed formed. The surface area of the nanofibers can be up to 100 cm^2, depending on the applied receiver of CA nanofibers during the electrospinning (see Fig. 2). In Fig. 2b, the obtained membranes consist of numerous randomly orientated nanofibers with a layer-by-layer network structure. Besides, the composite nanofibers have uniform dimension and smooth surface. The average diameter of the composite nanofibers is 336 nm (Fig. 3), being ultrafine but thick enough to encapsulate AgNC aggregates. In Fig. 2(c), a high density of AgNC aggregates are randomly distributed in CA nanofibers. Fig. 2(d) shows a high loading of aggregated AgNCs in CA nanofiber. In addition, Fig. 4 shows that the AgNCs

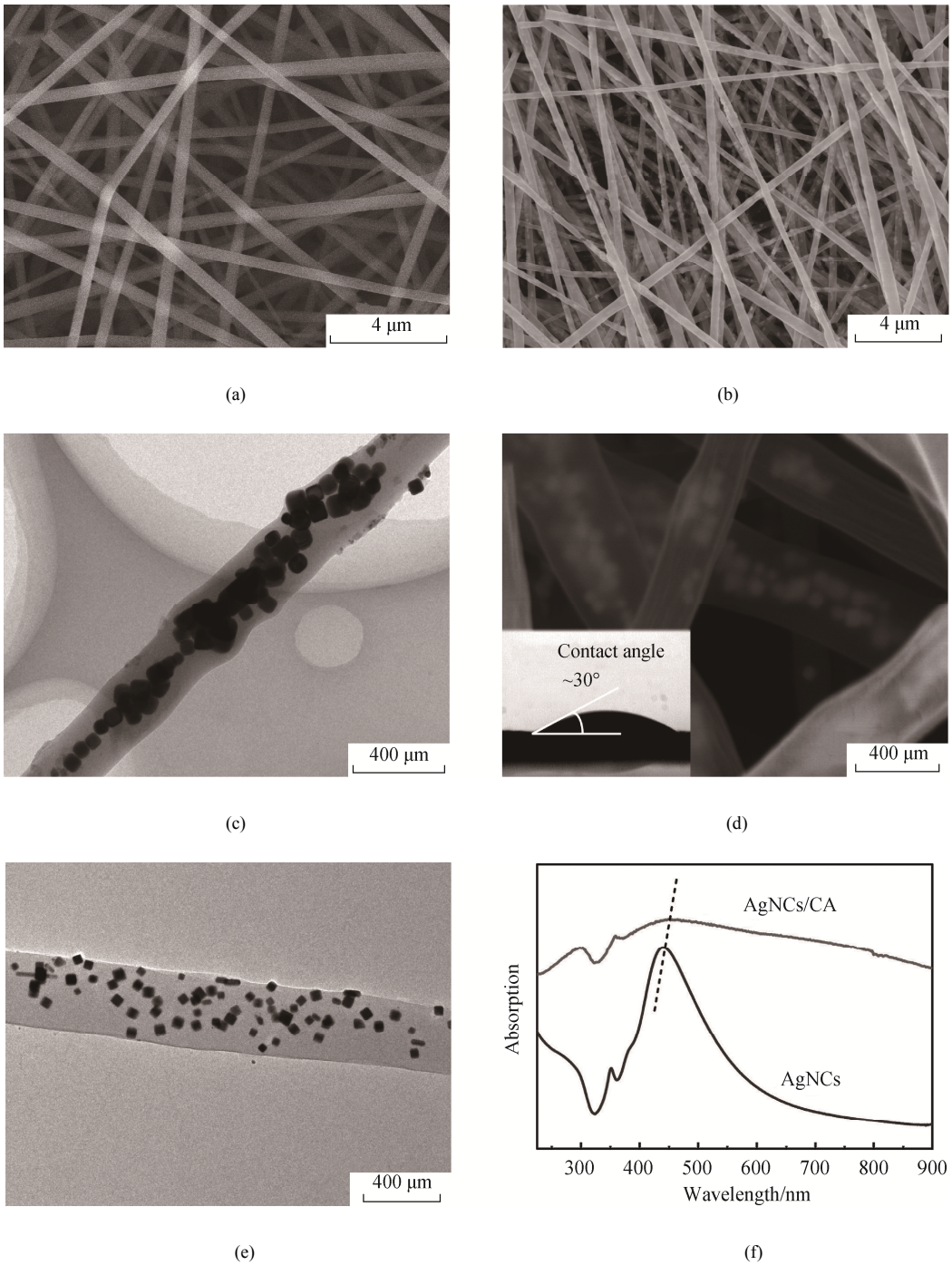


Fig. 2 Microscopic morphologies of the nanofibers: (a) SEM image of CA nanofibers electrospun from CA/acetone-DMAc solution; (b) SEM images of aggregated-AgNCs/CA nanofibers; (c) The corresponding close-up view of aggregated-AgNCs@CA nanofibers, the inset shows the water contact angle to be 30°; (d) and (e) are representative TEM images of AgNCs/CA nanofiber embedded with aggregated and monomeric AgNCs, respectively; and (f) UV–Vis spectra of the solution phase AgNCs and aggregated-AgNCs/CA membrane

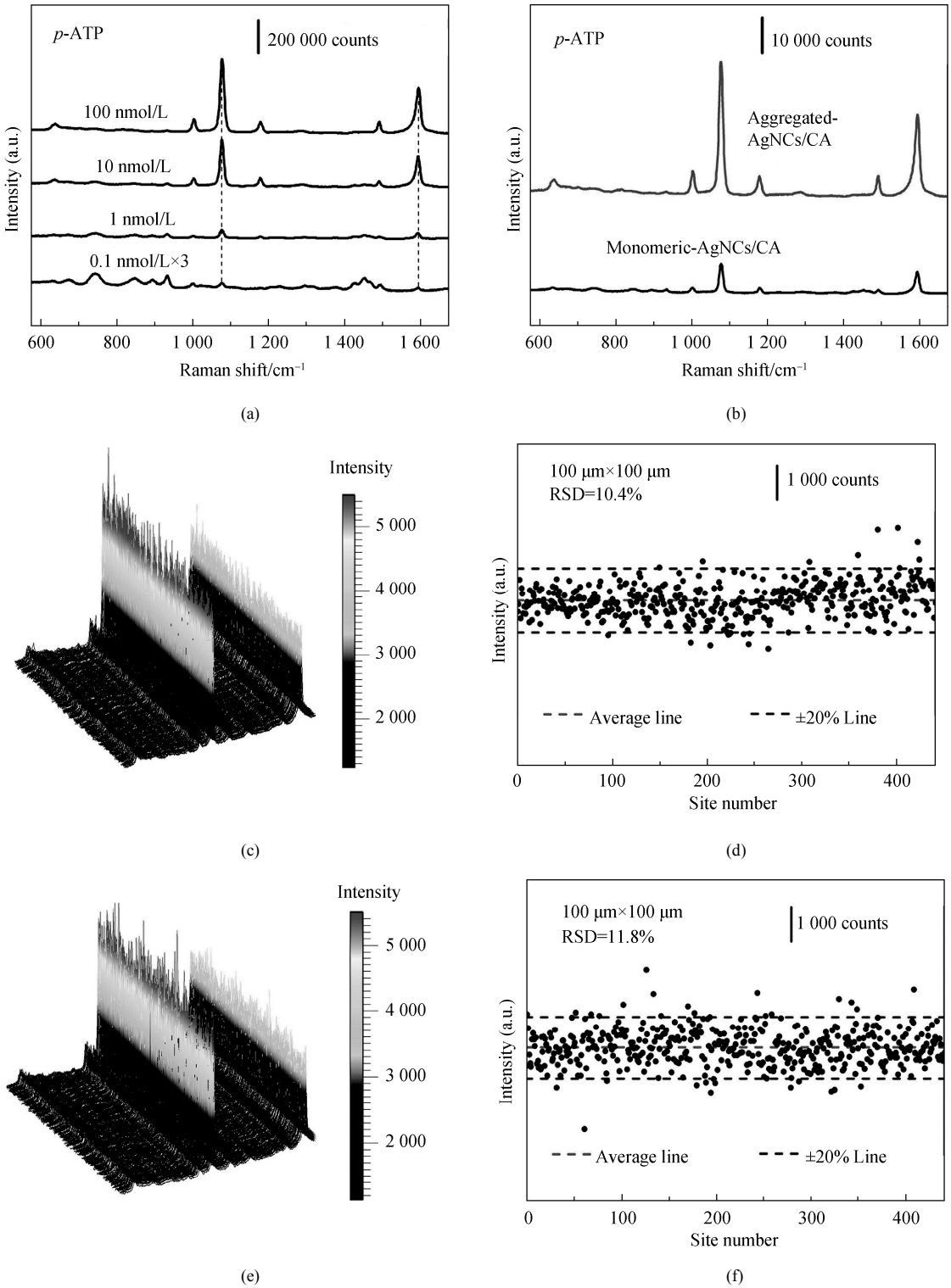


Fig. 3 (a) SERS spectra of *p*-ATP with different concentrations dispersed on aggregated-AgNCs/CA nanofibers; (b) SERS spectra of *p*-ATP (100 nM) adsorbed on aggregated-AgNCs/CA and monomeric-AgNCs/CA nanofibers, respectively; (c) SERS spectra (441 acquisions) of *p*-ATP recorded from aggregated-AgNCs@CA nanofibers with mapping area of 100 μm×100 μm, and (d) the corresponding intensity distribution of 1 078 cm^{-1} shift of *p*-ATP; (e) SERS spectra (441 acquisions) of *p*-ATP recorded from aggregated-AgNCs@CA nanofibers with mapping area of 1 mm×1 mm, and (f) the corresponding intensity distribution of 1 078 cm^{-1} shift of *p*-ATP

are in aggregated state, but electrospinning process does not make them grow larger. Note that a acetone-to-DMAc ratio plays a role in the aggregation degree of AgNCs. The excessive aggregation of AgNCs occurs when the acetone-to-DMAc ratio increases to 3/1, resulting in poor-quality nanofibers embedded with excessively

aggregated AgNCs (see Fig. S5). For comparison, monomeric AgNCs embedded in CA nanofibers were also fabricated by electrospraying AgNCs monodispersive CA/DMAc solution. In Fig. S6, each nanofiber is loaded with discontinuous AgNCs. In Fig. 2(e), the increase of loading ratio of AgNCs does not cause the aggregation of AgNCs. Fig. 2(f) demonstrates a broadened and slight red shift of SPR peak at 441-454 nm due to the collective plasmon coupling oscillation among coupled AgNCs[40].

3.3 SERS performance of the aggregated-AgNCs/CA nanofibers

It is well known that sub-10-nm gaps could be produced from Au/Ag NP aggregates and plenty of hotspots are generated for an ultrahigh Raman enhancement. It was reported that each hotspot of a NP dimer and trimer could even be 16 and 87 times as strong as a monomeric NP[41]. Therefore, aggregated-AgNCs/CA nanofibers show a high SERS activity. The SERS activities of aggregated-AgNCs/CA nanofibers were examined by using *p*-ATP as probe molecules. In Fig. 3(a), high-quality SERS fingerprint peaks of *p*-ATP at 1 078 cm^{-1} and 1 593 cm^{-1} appear even when the *p*-ATP concentration is 0.1 nmol/L, which is lower than that of reported electropspun SERS substrates embedded with sepatated AgNCs (1 nmol/L)[35] and cellulose-based SERS substrates wth Ag nanoparticles as active units (0.6 nmol/L)[42–43]. The average enhancement factor was calculated to be 3.8×10^6 (see Part S2). Note that the SERS signals of analytes with a low concentration (0.1 nmol/L) may merge with background Raman signals of PVP and CA, as shown in Fig.7. In addition, the SERS activity of aggregated-AgNCs/CA nanofibers was also compared with that of monomeric-AgNCs/CA nanofibers, as shown in Fig. 3(b). As expected, the SERS signals generated by CA nanofibers with AgNC aggregates are 4 times of greater than those by the monomeric one.

The uniformity of SERS substrate is also an important merit for practical application. To investigate the SERS signal uniformity of composite membranes, SERS mapping of *p*-ATP (100 nmol/L) recorded on a randomly selected area (100 μm×100 μm, step size of 5 μm, 441 measured points) from the aggregated-AgNCs/CA menbrane was performed. In Fig. 3(c), the SERS signals recorded from all 441 points are homogeneous. The distribution of peak intensities (1 078 cm^{-1} shift) from all the recorded SERS spectra is shown in Fig. 3(d), demonstrating a relative standard deviation (RSD) of 10.4%. As a SERS platform consisting of NPs, the presented RSD can be comparable with some nanostructure arrays. Moreover, even if the scaled mapping area is enlarged to 1 mm×1 mm (see Fig. 3(e)), large-area homogeneous SERS signals could still be achieved with a slightly increased RSD of 11.8% (see Fig. 3(f)).

The signal uniformity can be explained as follows: First, although AgNCs are not uniformly distributed in CA nanofibers due to AgNCs aggregation, the composite nanofibers with 3D layer-by-layer network structure appear homogeneous over a large area. A SERS spectrum is normally contributed from a plenty of composite nanofibers embedded with numerous random AgNC aggregates within laser focus (several μm^2, depending on the objective lens), thus being beneficial to generate relatively homogeneous SERS signals; Second, the distribution of molecules in the composite membranes should also be uniform due to the high homogeneity and hydrophility of the membranes. In this way, the homogeneous adsorption of target molecules can be realized.

3.4 Analytical application of the aggregated-AgNCs/CA nanofibers

MP is a highly toxic organophosphorous pesticide widely used for protecting the crops from insects. However, the extensive use of those organophosphorous pesticides makes them widely reside in soil, water environment and agricultural products, thus affecting human health and food safety. MP enters human body quickly and irreversibly inhibits the cholinesterases, leading to respiratory paralysis and even death. MP is thus classified by World Health Organization (WHO) under ‘Category Ia’ (extremely toxic) with the recommended maximum residue limit of MP range from 0.1 to 1.0×10^{-6}[44]. It is essential for rapid detection of trace-level MP in aqueous environmental samples. The vibrational modes of MP molecules were investigated by DFT included in a software named Gaussian 09W. A hybrid density functional B3LYP method with 6-31G/(d) basis set was used. A scale factor of 0.961 3 was used to correct the basis set superposition errors. Fig. 4(a) shows the optimized molecule structure and simulated Raman spectrum of MP. The main vibrational bands of MP locate at 1 089 cm^{-1} (C—N stretching), 1 213 cm^{-1} (C—O stretching), 1 344 cm^{-1} (C—N═O stretching), 1 464 cm^{-1} (C—H wagging), and 1 588 cm^{-1} (phenyl stretching), respectively.

In the case, MP molecules are difficult to be directly adsorbed on Ag surface. However, they should diffuse rapidly to the composite membranes, and especially to the hotspots of AgNCs inside CA fibers due to the hydrophilicity of AgNCs/CA nanofibers (water contact angle of ~30°). Fig. 4b shows the SERS spectra of MP with various concentrations by using aggregated-AgNCs/CA nanofibers as SERS substrates. The characteristic peaks at 858 cm^{-1} (O═N═O wagging), 1 111 cm^{-1} (C—N stretching), 1 348 cm^{-1}(C—N═O stretching) and 1 598 cm^{-1} (phenyl stretching) appear even at MP concentration of 10 nmol/L, demonstrating the composite membranes also have a high SERS sensitivity to the environmental organic pollutants. Besides, Fig. 4(c) shows a typical adsorption-saturation Langmuir relationship, indicating the SERS signals are also related to the adsorption behavior of the composite membranes towards the MP molecules. Moreover,

large-area homogeneous SERS signals of MP can be achieved with a low RSD~12.2% (see Fig. 4(f)), as proved by a large-area (1 mm×1 mm) SERS mapping in Fig. 4(d) and the corresponding 3D spectra view in Fig.4(e). It is thus indicated that aggregated-AgNCs/CA nanofiber membranes could be used as promising SERS substrates for trace detection of aqueous environmental organic pollutants.

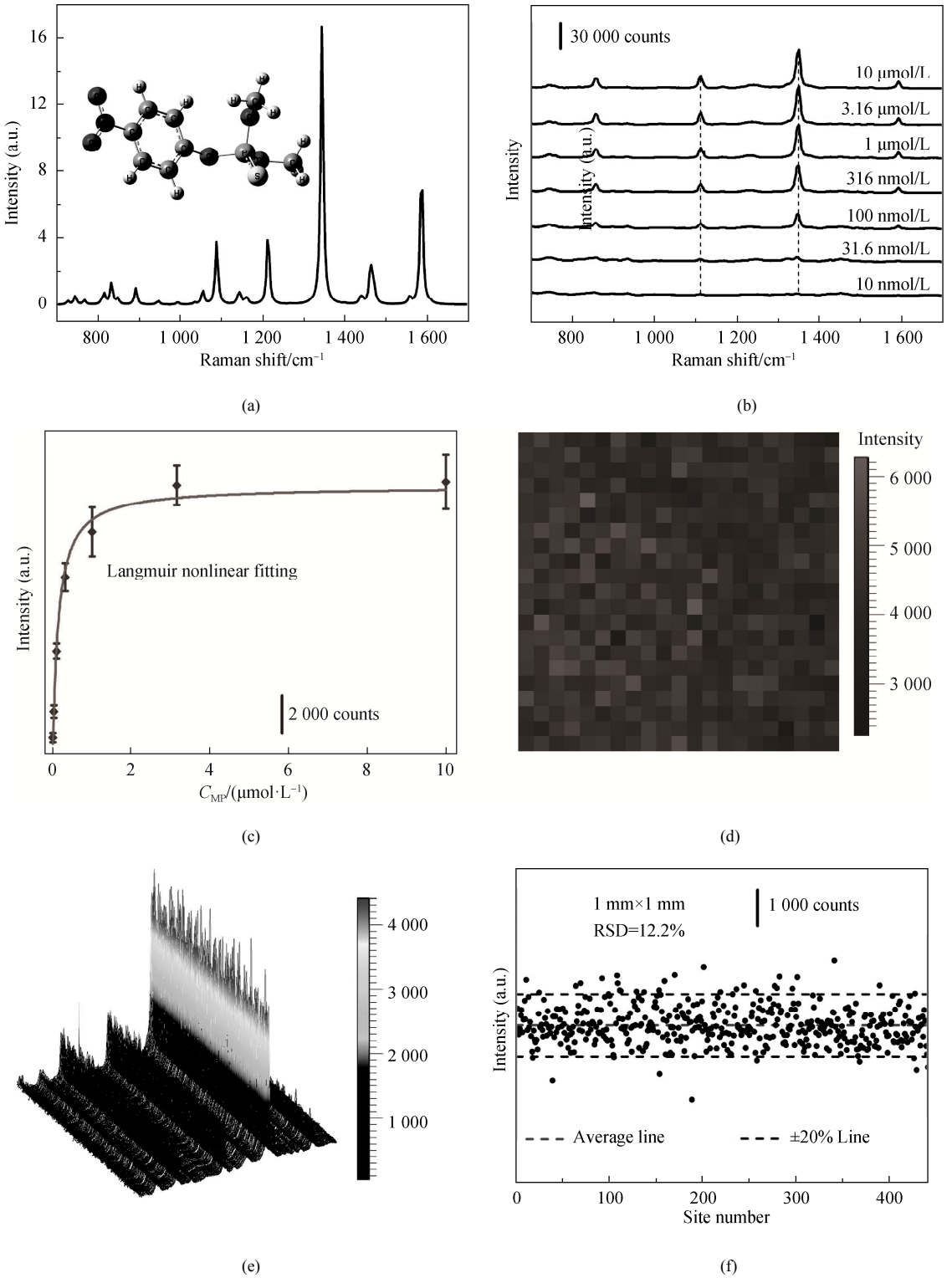


Fig. 4 (a) Simulated Raman spectrum of MP molecule and the optimized molecule structure (B3LYP/6-31+G(d)); (b) SERS spectra of MP aqueous solutions adsorbed on aggregated-AgNCs/CA nanofibers, and (c) the corresponding Langmuir nonlinear fitting of peak intensity at 1 111 cm^{-1} against the MP concentration; (d) SERS intensity mapping of 1 348 cm^{-1} shift of MP molecules measured from the aggregated-AgNCs@CA nanofibers (1 mm×1 mm, step size of 50 μm); (e) the 3D viewing of all 441 original SERS spectra; and (f) the intensity distribution of 1348 cm^{-1} peak of MP

4 Conclusions

Homogeneous CA nanofiber membranes with aggregated AgNCs were fabricated as reliable SERS substrates *via* co-electrospinning of AgNCs/CA/acetone-DMAc solution prepared by dispersing colloidal AgNCs in CA/acetone-DMAc (3/2) solution. Acetone served as a solvent of CA to form electrospinnable polymer solution and induced an appropriate aggregation of the AgNCs. The plasmonic nanofibers exhibited a superior SERS activity rather than nanofibers embedded with monomeric AgNCs due to the strong plasmon coupling between neighboring AgNCs in the aggregates. As a result, 0.1 nmol/L *p*-ATP and 10 nmol/L MP could be identified, respectively. Besides, the composite membranes could also generate large-area homogeneous SERS signals with RSD of *p*-ATP less than 12% in a 1 mm×1 mm area. It was indicated that aggregated-AgNCs/CA nanofibers could have a promising application for SERS-based rapid detection of trace-level organic pollutants in environmental aqueous solutions.

References:

[1] CLAVERO C. Plasmon-induced hot-electron generation at nanoparticle/metal-oxide interfaces for photovoltaic and photocatalytic devices[J]. Nat Photon, 2014, 8 (2): 95–103.

[2] WU N Q. Plasmonic metal-semiconductor photocatalysts and photoelectrochemical cells: a review[R]. Nanoscale, 2018, 10(6): 2679–2696.

[3] LEE S, SUN Y C, CAO Y Y, et al. Plasmonic nanostructure-based bioimaging and detection techniques at the single-cell level[R]. Trac-Trend Anal Chem, 2019, 117: 58–68.

[4] NAM J, WON N, JIN H, et al. pH-Induced aggregation of gold nanoparticles for photothermal cancer therapy[J]. J Am Chem Soc, 2009, 131(38): 13639–13645.

[5] ABADEER N S, MURPHY C J. Recent progress in cancer thermal therapy using gold nanoparticles[J]. J Phys Chem C, 2016, 120(9): 4691–4716.

[6] BEN HADDADA M, KOSHEL D, YANG Z, et, al. Proof of concept of plasmonic thermal destruction of surface cancers by gold nanoparticles obtained by green chemistry[J]. Colloid Surf B-Biointerfaces, 2019, 184: 1053708.

[7] ZHOU L, TAN Y L, WANG J Y, et al. 3D self-assembly of aluminium nanoparticles for plasmon-enhanced solar desalination[J]. Nat Photon, 2016, 10(6): 393–398.

[8] LINIC S, CHRISTOPHER P, INGRAM D B. Plasmonic-metal nanostructures for efficient conversion of solar to chemical energy[J]. Nat Mater, 2011, 10(12): 911–921.

[9] SHI R, Cao Y H, BAO Y J, et al. Self-assembled Au/CdSe nanocrystal clusters for plasmon-mediated photocatalytic hydrogen evolution[J]. Adv Mater, 2017, 29(27): 1700803.

[10] YIN H, LAN J G, GOUBERT G, et al. Nanoscale Surface Redox Chemistry Triggered by Plasmon-Generated Hot Carriers[J]. Small, 2019, 15(47): 1903674.

[11] SHAFER-PELTIER K E, HAYNES C L, GLUCKSBERG M R, et al. Toward a glucose biosensor based on surface-enhanced Raman scattering[J]. J Am Chem Soc, 2003, 125(2): 588–593.

[12] GAO X F, ZHENG P, KASANI S, et al. Paper-Based Surface-Enhanced Raman Scattering Lateral Flow Strip for Detection of Neuron-Specific Enolase in Blood Plasma[J]. Anal Chem, 2017, 89(18): 10104–10110.

[13] YANG S K, DAI X M, STOGIN B B, et al. Ultrasensitive surface-enhanced Raman scattering detection in common fluids[J]. PNAS, 2016, 113(2): 268–273.

[14] LE RU E C, BLACKIE E, MEYER M, et al. Surface enhanced Raman scattering enhancement factors: a comprehensive study[J]. J Phys Chem C, 2007, 111(37): 13794–13803.

[15] SUGANO K, AIB K, IKEGAM K, et al. Single-molecule surface-enhanced Raman spectroscopy of 4,4 '-bipyridine on a prefabricated substrate with directionally arrayed gold nanoparticle dimmers[J]. Jpn J Appl Phys, 2017, 56(6): 06GK01.

[16] HUANG Z L, MENG G W, HUANG Q, et al. Surface-enhanced Raman scattering from plasmonic Ag-nanocube@Au-nanospheres core@satellites[J]. J Raman Spectrosc, 2017, 48(2): 217–223.

[17] ZHANG D J, PENG L Q, SHANG X L, et al. Buoyant particulate strategy for few-to-single particle-based plasmonic enhanced nanosensors[J]. Nat Commun, 2020, 11(1): 2603.

[18] DONG X, GU H, KANG J, et al. Comparative study of surface-enhanced Raman scattering activities of three kinds of silver colloids when adding anions as aggregating agents[J]. Colloids Surfaces A-Physicochem Eng Aspects, 2010, 368: 142–147.

[19] JIANG T, WANG X L, ZHOU J, et al. The construction of silver aggregate with inbuilt Raman molecule and gold nanowire forest in SERS-based immunoassay for cancer biomarker detection[J]. Sensors Actuators B-Chem, 2018, 258: 105–114.

[20] OUHIBI A, SAADAOUI M, LORRAIN N, et al. Application of Doehlert Matrix for an Optimized Preparation of a Surface-Enhanced Raman Spectroscopy (SERS) Substrate Based on Silicon Nanowires for Ultrasensitive Detection of Rhodamine 6G[J]. Appl Spectrosc, 2020, 74(2): 168–177.

[21] MA Y, DU Y, CHEN Y, et al. Intrinsic Raman signal of polymer matrix induced quantitative multiphase SERS analysis based on stretched PDMS film with anchored Ag nanoparticles/Au nanowires[J]. Chem Eng J, 2020, 381: 122710.

[22] ALBA M, PAZOS-PEREZ N, VAZ B, et al. Macroscale plasmonic substrates for highly sensitive surface-enhanced raman scattering[J]. Angew Chem Int Ed, 2013, 52(25): 6459–6463.

[23] THIBAUT T, ZHENG Y, NG S H, et al. Self-assembly of vertically aligned gold nanorod arrays on patterned substrates[J]. Angew Chem Int Ed, 2012, 51(35): 8732–8735.

[24] ZHANG C L, LV K P, CONG H P, et al. Controlled assemblies of gold nanorods in PVA nanofiber matrix as flexible free-standing SERS substrates by electrospinning[J]. Small, 2012, 8(5): 648–653.

[25] WANG M, LI R, FENG X, DANG C, et al. Cellulose nanofiber-reinforced ionic conductors for multifunctional sensors and

devices[J]. ACS Appl Mater Interfaces, 2020, 12(24): 27545–27554.

[26] ISMAR E, SARAC A S. Electrospun polyacrylonitrile-lauric acid composite nanofiber webs as a thermal energy storage material[J]. J Eng Fibers Fabrics, 2019, 14: 1–6.

[27] SU S, LI J, ZHOU L, WAN S, et al. Ultra-thin electro-spun PAN nanofiber membrane for high-efficient inhalable PM2.5 particles filtration[J]. J Nano Res, 2017, 46: 73–81.

[28] BALACHANDAR V, MAHALAXMI I, KAAVYA J, et al. COVID-19: emerging protective measures[J]. Eur Rev Med Pharmacol Sci, 2020, 24(6): 3422–3425.

[29] ZHANG K, ZHANG L L, ZHAO X S, et al. Graphene/polyaniline nanofiber composites as supercapacitor electrodes[J]. Chem Mater, 2010, 22(4): 1392–1401.

[30] CHOI J, KIM W, LEE E, et al. Characterization of PU nanofiber web treated with non-oxidized graphene and silver nanowire[J]. Fibers Polym, 2020, 21(5): 978–983.

[31] LI L, DENG S, WANG H, et al. A SERS fiber probe fabricated by layer-by-layer assembly of silver sphere nanoparticles and nanorods with a greatly enhanced sensitivity for remote sensing[J]. Nanotechnology, 2019, 30(25): 255503.

[32] ZHANG C L, LV K P, HUANG H T, et al. Co-assembly of Au nanorods with Ag nanowires within polymer nanofiber matrix for enhanced SERS property by electrospinning[J]. Nanoscale, 2012, 4(17): 5348–5355.

[33] HUANG B, WANG Y, HU Q, et al. A low temperature and highly sensitive ethanol sensor based on Au modified In_2O_3 nanofibers by coaxial electrospinning[J]. J Mater Chem C, 2018, 6(40): 10935–10943.

[34] WU S, QIN X, LI M. The structure and properties of cellulose acetate materials: A comparative study on electrospun membranes and casted films[J]. J Ind Text, 2014, 44(1): 85–98.

[35] KE Y, MENG G, HUANG Z, et al. Electrosprayed large-area membranes of Ag-nanocubes embedded in cellulose acetate microspheres as homogeneous SERS substrates[J]. J Mater Chem C, 2017, 5(6): 1402–1408.

[36] SKRABALAK S E, AU L, LI X D, et al. Facile synthesis of Ag nanocubes and Au nanocages[J]. Nat Protoc, 2007, 9: 2182–2190.

[37] TUNGPRAPA S, PUANGPARN T, WEERASOMBUT M, et al. Electrospun cellulose acetate fibers: effect of solvent system on morphology and fiber diameter[J]. Cellulose, 2007, 14(6): 563–575.

[38] PULS J, WILSON S A, HOELTER D. Degradation of cellulose acetate-based materials: A review[J]. J Polym Environ, 2011, 19(1): 152–165.

[39] MOGHE A K, GUPTA B S. Co-axial electrospinning for nanofiber structures: Preparation and applications[J]. Polym Rev, 2008, 48(2): 353–377.

[40] GILROY K D, XIA Y. Dimerization of colloidal particles through controlled aggregation for enhanced properties and applications[J]. Chem Asian J, 2016, 11(17): 2341–2351.

[41] CHEN G, WANG Y, YANG M, et al. Measuring Ensemble-Averaged surface-enhanced raman scattering in the hotspots of colloidal nanoparticle dimers and trimers[J]. J Am Chem Soc, 2010, 132(11): 3644–3645.

[42] LI Y X, ZHANG K, ZHAO J J, et al. A three-dimensional silver nanoparticles decorated plasmonic paper strip for SERS detection of low-abundance molecules[J]. Talanta, 2016, 147: 493–500.

[43] LEE M, OH K, CHOI H K, et al. Subnanomolar sensitivity of filter paper-based sers sensor for pesticide detection by hydrophobicity change of paper surface[J]. ACS Sensors, 2018, 3(1): 151–159.

[44] MISHRA A, KUMAR J, MELO J S. An optical microplate biosensor for the detection of methyl parathion pesticide using a biohybrid of Sphingomonas sp cells-silica nanoparticles[J]. Biosens Bioelectro, 2017, 87: 332–338.